JOURNAL OF APPLIED POLYMER SCIENCE VOL. 21, 1045–1055 (1977)

# Morphological Studies of Poly(olefin Sulfones) by Light Scattering*

W. H. CHU, E. GIPSTEIN, and A. C. OUANO, *IBM Research Laboratory, San Jose, California 95193*

## Synopsis

Poly(olefin sulfones) are readily degraded by an electron beam and thus could be used as electron beam resists. However, films greater than 3000 Å thick crack during formation and especially during solvent development following exposure to an electron beam. As crystallinity accentuates cracking owing to swelling stresses at the crystalline–amorphous interface, the morphology of various poly(olefin sulfones) was studied by light scattering. Materials investigated were solvent-cast and hot-pressed films of poly(butene-1 sulfone) (PBS), poly(cyclopentene sulfone) (PCPS), poly(bicycloheptene sulfone) (PBCHS), and two terpolymers of poly(cyclopentene sulfone–*co*–butene-1 sulfone), in which the molar ratios of cyclopentene to butene-1 were 50/50 (TP1) and 70/30 (TP2). All hot-pressed samples showed scattering patterns characteristic of randomly oriented rod-like superstructures 8–10 $\mu$m in length. Among the solvent-cast films, however, only PBS and TP2 samples scattered light indicative of crystallinity. Scattering from these samples was analyzed in terms of "random orientation fluctuation" light scattering theory. Correlation distances of 1.7 and 1.5 $\mu$m for the PBS and TP2, respectively, were obtained. The solvent-cast crystalline films (PBS and TP2) had a tendency to crack during dissolution as did the amorphous films of PCPS and PBCHS, indicating that cracking depends on the glass temperature as well as crystallinity. Only the amorphous terpolymer TP1 did not crack, presumably owing to its relatively low glass temperature effected by the butene-1 moiety.

## INTRODUCTION

The film properties of poly(olefin sulfones) have been examined to determine their potential as electron beam resists.[1–4] In general, the quality of many of the films from these polymers was marginal, especially those from cycloaliphatic sulfones, which showed a high tendency to crack in solvents. Baking these films above their $T_g$ to relieve stresses reduced the tendency to crack, but the cracking was not entirely eliminated. Stress-relieved thin films of poly(cyclopentene sulfone) (PCPS) and poly(bicycloheptene sulfone) (PBCHS) did not crack, but films thicker than 3000 Å cracked in solvents during development.[3] Presumably, physical properties such as the glass transition temperature and the crystallinity could be factors responsible for the cracking. Thus, polymers with high $T_g$'s often crack during film formation from solution and during dissolution due to swelling stresses. Crystallinity can cause a constrained swelling of the amorphous regions at the crystalline–amorphous interface, thus producing swelling stresses which result in crack formation at a temperature below the $T_g$ of the

* Presented at the First Chemical Congress of North American Continent, Mexico City, Mexico, November 30 to December 5, 1975.

TABLE I
Some Physical Properties of Poly(olefin Sulfones)[a]

| Sample | $T_c$, °C | $T_g$, °C | Crystallinity in solvent-cast film | Cracking during film formation | Cracking during dissolution |
|---|---|---|---|---|---|
| PBS | 64 | 81 | yes | no | yes |
| PCPS | 103 | 82 | no | yes | — |
| PBCHS | 150 | 117 | no | yes | — |
| TP1 | 74 | 57 | no | no | no |
| TP2 | — | 74 | yes | no | yes |

[a] $T_c$: Ceiling temperature; $T_g$: glass transition temperature.

polymer. Both of these factors appear to be important for poly(olefin sulfones), since their $T_g$'s are generally above room temperature, and some show evidence for crystallinity.[5]

In the present study, solution-cast and hot-pressed films from the above-indicated poly(olefin sulfones) were studied by light scattering. Results were compared with theoretical calculations using light scattering theory for structure identification. Photomicroscopy and scanning electron microscopy (SEM) measurements were also carried out. The structure/property relationship for these poly(olefin sulfones) was qualitatively evaluated.

## EXPERIMENTAL

### Materials

Poly(butene-1 sulfone) (PBS), poly(cyclopentene sulfone) (PCPS), poly(bicycloheptene sulfone) (PBCHS), and two terpolymers, poly(cyclopentene sulfone–*co*–butene-1 sulfone) with molar ratios of 50/50 (TP1) and 70/30 (TP2) as reported[3] were synthesized. Film samples were prepared by solution casting and by hot-pressing techniques. In the solution casting procedures, a 10% solution by weight of the polymer in nitromethane was prepared for each material except for PCPS, which was dissolved in 1,3-dichloropropane. The solutions were filtered through a fine porosity glass filter and then poured into a flat-bottom Petri dish and covered with a glass plate having a small hole in the center. The solution was allowed to evaporate slowly for at least two days until a visually dry film was formed which was then placed in a vacuum oven at 50°C for 1 hr to remove residual solvent. The films were about 0.2 mm thick.

For the hot-pressed samples, the polymer powders were placed on a hot press at a temperature of 120°C and a pressure of $1.38 \times 10^8$ N/m$^2$ for 2 hr and then allowed to cool to room temperature. The press temperature was higher than the decomposition temperature of some of the materials (cf., Table I); however, no decomposition (as evidenced by the yellowing of the film) was observed from the pressed films. Presumably, the presence of pressure caused a shift of the decomposition temperature toward a higher temperature.[6] The pressed samples were about 2.0 mm thick.

### Light Scattering

Photographic and photometric scattering experiments were carried out. A typical photographic light scattering apparatus was used to record both $H_v$ (vertically polarized incident beam, horizontally oriented analyzer) and $V_v$ (vertically polarized incident beam, vertically oriented analyzer) patterns. The light source was a Spectra Physics Model 133-01 helium–neon laser equipped with a Spectra Physics polarization rotator whose power and wavelength are 1.0 milliwatt and 632.8 nm, respectively. The scattering patterns were recorded on Polaroid Type 52 film, ASA 400. Specimens were mounted between a 2.5 × 7.5 cm microscope slide and a 2.2 × 2.2 cm Corning cover glass with matching refractive index fluid to eliminate any surface scattering.

The photometric apparatus has been described elsewhere.[7] The samples which scattered light as observed in the photographic experiment were studied by a photometric method. The scattered light intensity from the hot-pressed samples was measured along radial scattering angles with polarizer and analyzer at +45° and −45°, respectively. For the solution-cast samples, the polarizer was at 0° and the analyzer at 90°. All required corrections[8] were performed on the collected data.

### Microscopy

The fracture surface of the hot-pressed samples was studied on a Kent Cambridge Model S-4 scanning electron microscope. The fracture surface was coated with a 200-Å-thick layer of palladium gold; the voltage of the electron beam was at 10 Kv. Photomicrographs of samples were taken with a polarizing microscope under cross polarization. The dissolution behavior was also examined with a polarizing microscope.

### Glass Transition Temperature Determination

The glass transition temperatures ($T_g$'s) were determined with a dilatometer having a sample bulb of 2 ml volume and a 60-cm-long capillary tube with an inner diameter of 0.5 mm. Mercury was mixed with the sample, and the sample bulb was immersed in a temperature-controlled silicone oil bath for heating and cooling. Changes in volume were measured on a fine graduated scale placed adjacent to the capillary tube. Data were taken during both heating and cooling paths to assure the reproducibility of the $T_g$ measurements.

## RESULTS AND DISCUSSION

Photographic scattering experiments showed that all hot-pressed samples scattered light and gave similar $H_v$ and $V_v$ scattering patterns as represented in Figure 1. The $H_v$ pattern showed the characteristic scattering for randomly oriented rod-like structures with the main polarizability direction parallel to the long rod axis[9] as had been observed for amylose films.[10] However, the observed $V_v$ pattern of the type found has not been reported.

According to the light scattering theory for a randomly oriented rod-like

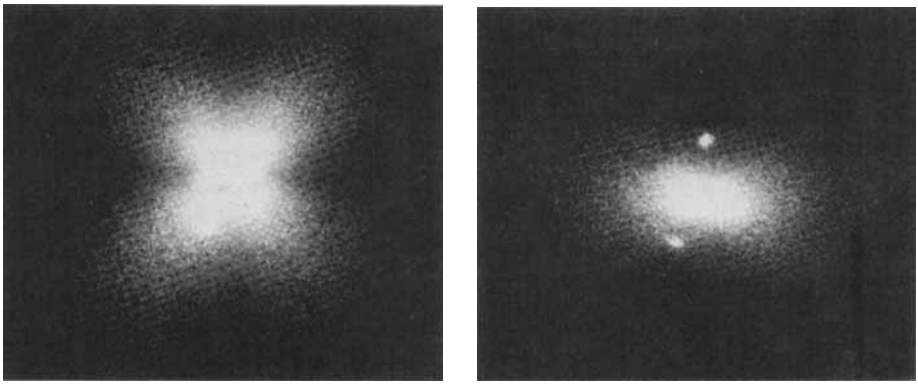

(a) (b)

Fig. 1. Light scattering patterns from hot-pressed films of poly(olefin sulfones); (a) $H_v$; (b) $V_v$.

structure, the $H_v$ and $V_v$ scattering intensity can be expressed by[9]

$$I_{H_v} = \rho_0^2 N_0 L^2 \int_0^{\pi} \delta^2 \sin^2 \alpha \cos^2 \alpha \left[\frac{\sin (kaL/2)}{(kaL/2)}\right]^2 d\alpha \tag{1}$$

and

$$I_{V_v} = \rho_0^2 N_0 L^2 \int_0^{\pi} (\delta \cos^2 \alpha + b_t)^2 \left[\frac{\sin (kaL/2)}{(kaL/2)}\right]^2 d\alpha \tag{2}$$

where $a = -\sin(\alpha + \mu) \sin \theta$; $\mu$ and $\theta$ are the azimuthal and radial angles of the scattered lights, respectively; $\alpha$ denotes the orientation of the rod; $\rho_0$ is the scattering power of a rod per unit length per unit incident field strength when the rod is oriented at $\alpha = 0°$; $N_0$ is the total number of rods; $k = 2\pi/\lambda$, where $\lambda$ is the wavelength of light in the medium; $\delta$ is the polarizability anisotropy of the rod; $b_t$ is the difference between the polarizability in the transverse direction to the long axis of the rod and that of the surrounding; and $L$ is the length of the rod. According to eq. (1), the $\delta$ of the rod affects only the overall intensity but not the angular dependence of the scattered light. However, from eq. (2), the $\delta$ and $b_t$ can strongly affect the overall $V_v$ pattern as shown in the theoretically calculated scattering patters from randomly distributed rods of different $\delta$ and $b_t$ (Fig. 2).

These two parameters were adjusted, and Figure 3 shows the calculated $H_v$ and $V_v$ patterns when $\delta = 1$ and $b_t = 2$, in good agreement with the experimentally observed patterns shown in Figure 1. The values of $\delta$ and $b_t$ are arbitrary units, but can be used to provide information on the packing of the chains if the polarizabilities of the chains are known. The fact that all the hot-pressed samples showed similar scattering patterns suggests that the same type of superstructure is formed in these materials when they are crystallized under pressure at high temperature. The extended birefringent structures in the hot-pressed samples are shown in the photomicrograph taken between crossed polaroids (cf., Fig. 4). The fracture surface of a hot-pressed sample showing the stacking of the crystalline structures is shown in Figure 5.

The size of these rod-like domains cannot be determined from the photographic $H_v$ scattering pattern, since there is no intensity maximum away from

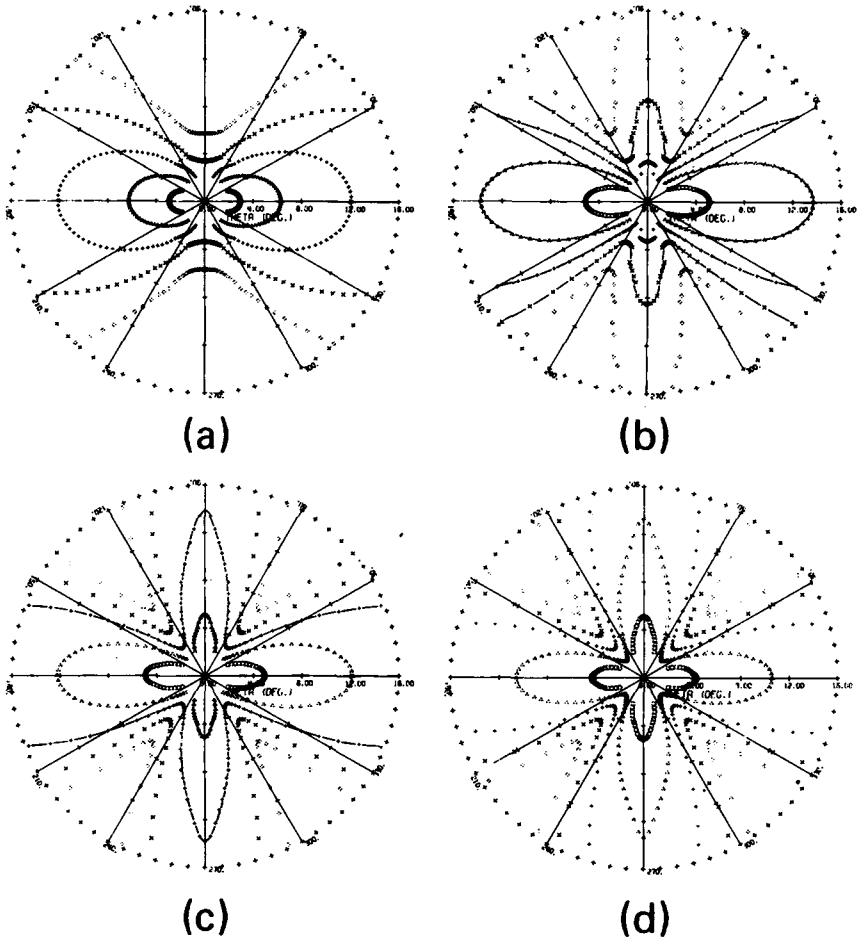


Fig. 2. Calculated $V_v$ scattering patterns from randomly oriented rod-like structures; (a) $\delta = 2.0$, $b_t = 1.0$; (b) $\delta = 4.0$, $b_t = -1.0$; (c) $\delta = 5.0$, $b_t = -2.0$; (d) $\delta = 6.0$, $b_t = -3.0$.

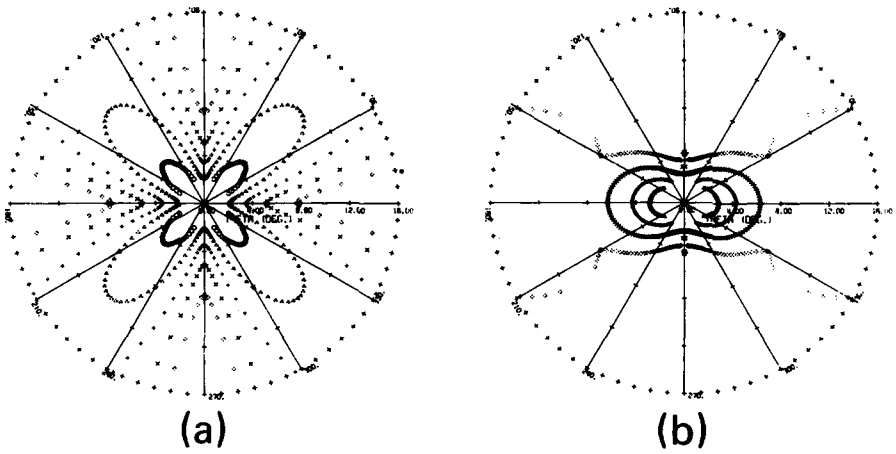


Fig. 3. Calculated scattering patterns from randomly oriented rod-like structures with $\delta = 1.0$, $b_t = 2.0$ and $L = 10$ $\mu$m; (a) $H_v$; (b) $V_v$.

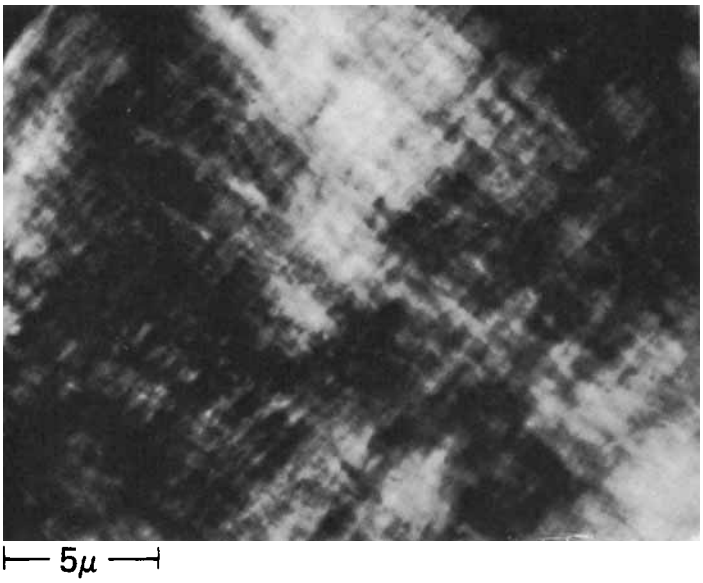


Fig. 4. Photomicrograph of hot-pressed poly(olefin sulfones) in-between crossed polaroids.

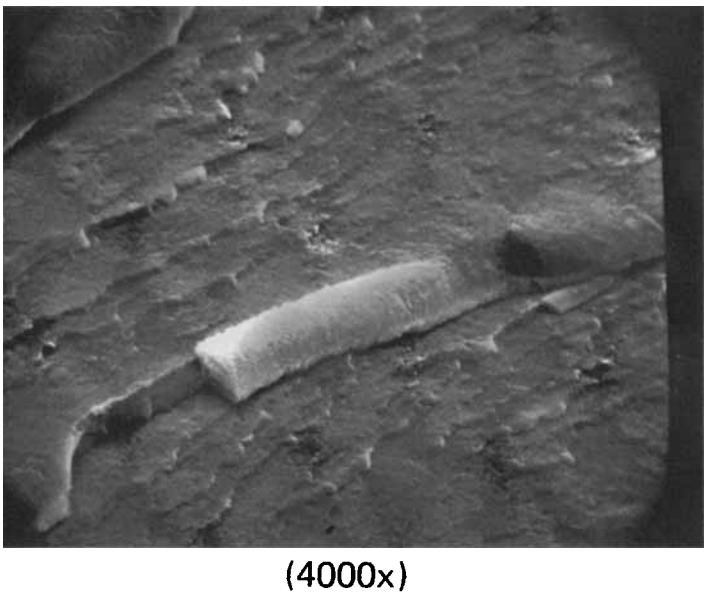


Fig. 5. Electron micrograph of fractured surface of hot-pressed poly(olefin sulfones).

the incident beam in the four-lobe pattern. This is in contrast to spherulitic scattering patterns where a scattering maximum can be related to the average size of the spherulites. An absolute scattering intensity measurement cannot yield any information about the size unless all the physical constants such as $\rho_0$, $N_0$, and $\delta$ in eq. (1) are known. However, the scattering ratio variations (with respect to the scattering at a reference scattering angle) with $\theta$'s are characteristically associated with the size because all other physical constants in eq. (1) are canceled when a ratio is taken.

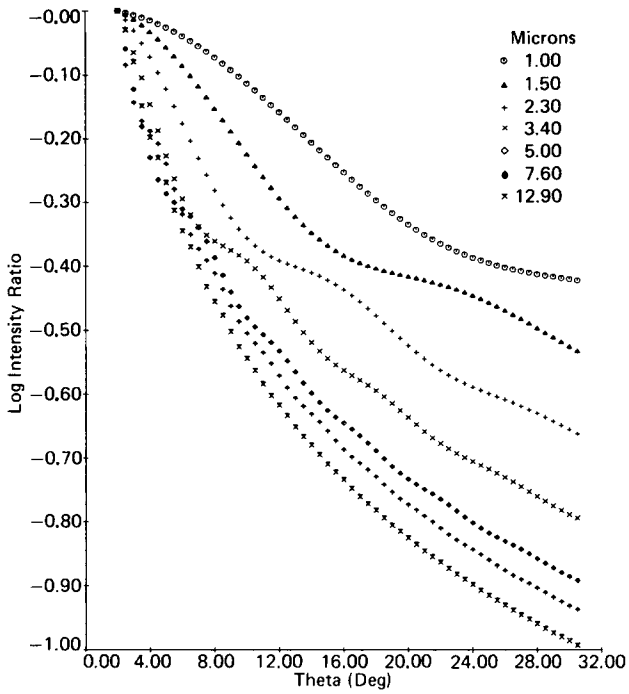


Fig. 6. Calculated $H_v$ intensity ratio from randomly oriented rod-like structures of different sizes.

Theoretical calculations of $H_v$ intensity ratio variations (reference angle at $\mu = 45°$ and $\theta = 2°$) with $\theta$'s at $\mu = 45°$ for randomly oriented rods of different lengths are shown in Figure 6. The photometrically measured scattering intensities from the hot-pressed samples were used to calculate the intensity ratios $(I_\theta/I_{2°})_{\mu=45°}$ and were compared with the theoretical curves. The comparison showed that the length of the rods in these samples was in the range of 8–10 $\mu$m, although some deviations were observed, especially at large scattering angles. Rods may have internal disorder due to the inclusion of amosphous regions inside the rod and in-between rods which would cause the deviations at small and large angles.[11] These deviations did not change appreciably the overall curve comparison, and the size estimated from the light scattering experiment agreed well with that observed in the photomicrograph.

For the five solvent-cast samples, only PBS and TP2 scattered light and gave $H_v$ scattering patterns, as shown in Figure 7. The cylindrically symmetrical pattern is characteristic of light scattered by anisotropic crystallites possessing randomly correlated orientation fluctuations.[12] The $H_v$ intensity from such a system can be expressed by[12]

$$I_{H_v} = \frac{64\pi^5}{\lambda_0^4}\delta^2 \int_0^r f(r)\frac{\sin hr}{hr} r^2\, dr \tag{3}$$

where $h = 2k \sin(\theta/2)$, $\lambda_0$ is the wavelength of light in vacuum, $\delta$ is the average optical anisotropy, and $f(r)$ is a correlation function defined by

$$f(r) = [3\langle \cos^2 \theta_{ij} \rangle_{r_{ij}} - 1]/2 \tag{4}$$

(a)

(b)

Fig. 7. $H_v$ scattering patterns from solvent-cast poly(olefin sulfones); (a) PBS; (b) TP2.

where $\theta_{ij}$ is the angle between the optic axes of scattering elements $i$ and $j$ separated by a distance of $r_{ij}$. This function decreases from unity at $r_{ij} = 0$ (indicating perfect correlations) toward zero as $r_{ij}$ becomes large. The detailed form of the variations is dependent upon the structure of the system. The distance over which the decrease occurs is a measure of the size of the correlated regions. The correlation function can be obtained by a Fourier inversion of eq. (3), and for many materials it can be represented by an empirical function

$$f(r) = \exp(-r/a) \tag{5}$$

or

$$f(r) = \exp(-r^2/a^2) \tag{6}$$

where $a$ is the correlation distance.

The $H_v$ intensity variations with $\theta$ for PBS and TP2 were measured from 0.5° to 25.0°. By the Fourier inversion, it was found that the orientation correlation function for the two samples could be represented by eq. (6) as shown in Figure

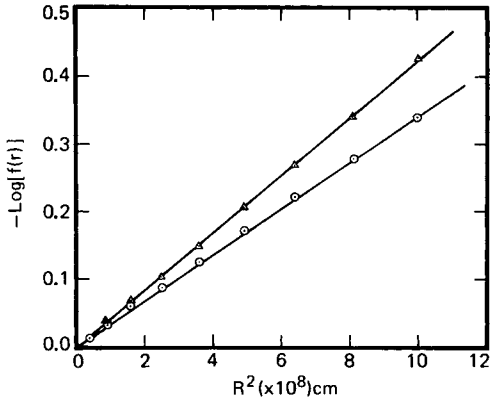


Fig. 8. Variation of $-\log [f(r)]$ with $r$ for (▲) PBS and (⊙) TP2.

8. The correlation distances obtained from the slopes of the two straight lines were 1.7 $\mu$m for PBS and 1.5 $\mu$m for TP2. These results indicate that PBS was the only crystallizable copolymer. The introduction of a noncrystallizing component, PCPS, into the terpolymer TP2 reduced the size of the crystalline domains. However, TP1, which contained less of the noncrystallizing component, showed no crystallinity. This anomaly might depend on the polymer–solvent interaction, a dominant factor in solvent-induced crystallization.

A distinct difference in morphology between the hot-pressed and solvent-cast samples was observed. The hot-pressed samples were crystalline and contained large superstructures. The solvent-cast samples, except for PBS and TP2, were noncrystalline.

During the hot-pressing process, the polymer macromolecules may be capable of packing into a thermodynamically lower energy state, i.e., crystalline, due to the presence of pressure at a temperature above the $T_g$ of the material. The crystallites formed may in turn develop into larger superstructures, in this case, long regions of rod-like structures. Pressure-induced crystallization of polymers has been observed.[13] Therefore, the differences in morphology might be attributed to the different methods used in preparing the polymer films.

The $T_g$'s and other physical properties of these poly(olefin sulfones) are tabulated in Table I. It is of interest to note that the two terpolymers, TP1 and TP2, have lower $T_g$'s than either PBS and PCPS.

For many copolymers, the $T_g$ lies between the $T_g$ of the constituting components,[14] although deviations from this general relationship have been observed.[15–17] Terpolymerization can lower the $T_g$, owing to internal plasticization by the side chain and a diminution in the concentration of sulfone groups.[5] The lowering of the $T_g$ observed in TP1 and TP2 can presumably be attributed to such an internal plasticization effect. The effectiveness of this internal plasticization appears to be composition dependent as a maximum lowering of $T_g$ was observed in TP1.

The two high-$T_g$ samples, PCPS and PBCHS, cracked during film formation. The cracking can be attributed to the stress build-up as some swollen regions in the solution become glassy during solvent evaporation. The stress, dependent on the $T_g$ of the material, can exceed the ultimate strength of the material if the $T_g$ is much higher than the solution temperature and thus causes cracking.

The dissolution of polymers can be classified as either normal (class I) or "anomalous" (class II).[18] In normal dissolution, a gel layer is present which can heal cracks and holes created by the penetration of the solvent and the polymer dissolves without cracking. In the class II process, polymers dissolve without forming a clearly defined gel layer. Thus, the swelling stress generated during dissolution cannot be dissipated resulting in cracking. Polymers such as poly(methyl methacrylate) dissolve normally near the $T_g$ and can change to a class II process with a progressive decrease in temperature.[19] The presence of crystallinity can also accentuate cracking owing to the swelling stress at the crystalline–amorphous interface.

The two polysulfones, PBS and TP2, which cracked during dissolution have either a high $T_g$ or are crystalline. The only sample that did not crack either during film formation or dissolution was TP1, which was amorphous and had a low $T_g$. All the samples were also studied by light scattering during dissolution to check for solvent-induced crystallization which might contribute to cracking. These results were negative. Thus, the cracking observed in these samples must be associated with the high $T_g$ and/or the crystallinity in the polymers.

## CONCLUSIONS

Morphological data obtained on five poly(olefin sulfones) by light scattering and microscopy studies indicate that the structures formed in these samples depend upon the sample preparation method. All hot-pressed film samples contain large crystalling rod-like structures in the range of 8–10 $\mu$m in length. These long structures are presumably lying parallel to the plane of the film. For films prepared by solvent casting, PB1 and TP2 contain randomly oriented crystalline domains averaging 1.7 and 1.5 $\mu$m in size, respectively. The smaller size domains observed in TP2 are due to the inclusion in the polymer of the noncrystallizing cyclopentene sulfone component. The overall composition of the terpolymer appears to determine the crystallizability of the polymer.

The cracking of these films is attributed to a high $T_g$. Crystallinity might also be a factor contributing to the cracking. Terpolymerization can effectively plasticize the polymer, thus lowering the $T_g$ and reducing the cracking.

## References

1. M. Bowden and L. Thompson, *J. Appl. Polym. Sci.*, **17**, 3211 (1973).
2. R. Himics, M. Kaplan, N. Desai, and E. Poliniak, *Coating and Plastics*, **35**(2), 266 (1975).
3. E. Gipstein, W. Moreau, G. Chiu, and O. Need, *J. Appl. Polym. Sci.*, **21**, 677 (1977).
4. M. Bowden and E. Chandross, *J. Electrochem. Soc.*, **122**, 1370 (1975).
5. K. J. Ivin and J. B. Rose, *Advan. Macromol. Chem.*, **1**, 335 (1968).
6. A. H. Frazer, *J. Polym. Sci.* **3**, 3699 (1965).
7. W. H. Chu, to be submitted.
8. R. S. Stein and J. J. Keane, *J. Polym. Sci.*, **17**, 21 (1955).
9. M. B. Rhodes and R. S. Stein, *J. Polym. Sci. A2*, **7**, 21 (1969).
10. J. E. Unbehend and A. Sarko, *J. Polym. Sci., Phys.*, **12**, 545 (1974).
11. T. Hashimoto, Y. Murakami, N. Hayashi, and H. Kawai, *Polym. J.*, **6**, 132 (1974).
12. R. S. Stein and P. R. Wilson, *J. Appl. Phys.*, **33**, 1914 (1962).
13. B. Wunderlich and T. Davidson, *J. Polym. Sci. A2*, **7**, 2043 (1969).
14. M. Gordon and J. S. Taylor, *J. Appl. Chem.*, **2**, 493 (1952).
15. R. B. Beevers and E. T. White, *Trans. Faraday Soc.*, **56**, 1529 (1960).

16. R. B. Beevers, *Trans. Faraday Soc.*, **58,** 1465 (1962).
17. K. H. Illers, *Kolloid Z.*, **190,** 16 (1963).
18. K. Ueberreiter, *Diffusion in Polymers,* J. Crank and G. S. Park, Eds., Academic Press, New York, 1968.
19. F. Asmussen and G. Raptis, Diplomarbeit, Freie Universität-Berlin, 1965.

Received March 17, 1976
Revised April 6, 1976